



# Potential of neuronal activity by tonic GluD1 current in brain slices

Daniel S Copeland, Aleigha Gugel & Stephanie C Gantz\* 

## Abstract

Ion channel function of native delta glutamate receptors (GluD<sub>R</sub>) is incompletely understood. Previously, we and others have shown that activation of G $\alpha_q$  protein-coupled receptors (GqPCR) produces a slow inward current carried by GluD<sub>1R</sub>. GluD<sub>1R</sub> also carries a tonic cation current of unknown cause. Here, using voltage-clamp electrophysiological recordings from adult mouse brain slices containing the dorsal raphe nucleus, we find no role of ongoing G-protein-coupled receptor activity in generating or sustaining tonic GluD<sub>1R</sub> currents. Neither augmentation nor disruption of G protein activity affects tonic GluD<sub>1R</sub> currents, suggesting that ongoing G-protein-coupled receptor activity does not give rise to tonic GluD<sub>1R</sub> currents. Further, the tonic GluD<sub>1R</sub> current is unaffected by the addition of external glycine or D-serine, which influences GluD<sub>2R</sub> current at millimolar concentrations. Instead, GqPCR-stimulated and tonic GluD<sub>1R</sub> currents are regulated by physiological levels of external calcium. In current-clamp recordings, block of GluD<sub>1R</sub> channels hyperpolarizes the membrane by ~7 mV at subthreshold potentials, reducing excitability. Thus, GluD<sub>1R</sub> carries a G-protein-independent tonic current that contributes to subthreshold neuronal excitation in the dorsal raphe nucleus.

**Keywords** cation channel; delta glutamate; G protein; GluD; tonic current

**Subject Category** Neuroscience

**DOI** 10.15252/embr.202356801 | Received 9 January 2023 | Revised 19 April 2023 | Accepted 24 April 2023 | Published online 8 May 2023

**EMBO Reports (2023) 24: e56801**

## Introduction

The majority of excitatory neurotransmission in the central nervous system is produced by ionic current carried by the ionotropic glutamate receptors (iGluRs). Lesser known in the iGluR family are the delta glutamate receptors (GluD<sub>1R</sub> and GluD<sub>2R</sub>), which share < 30% amino acid sequence identity with the other family members (Araki *et al.*, 1993; Lomeli *et al.*, 1993). Either GluD<sub>1R</sub> or GluD<sub>2R</sub> is expressed in the central neurons in nearly every region of the adult mouse brain, with a high level of overlap at the regional and cellular level (Konno *et al.*, 2014; Hepp *et al.*, 2015; Nakamoto *et al.*, 2020). Predominately, GluD<sub>1R</sub> and GluD<sub>2R</sub> are found in postsynaptic

specializations on the dendrites and spines (Landsend *et al.*, 1997; Hepp *et al.*, 2015; Nakamoto *et al.*, 2020; Hoover *et al.*, 2021), where they regulate synapse formation, composition, and autophagy in complex with trans-synaptic and secreted proteins (Tao *et al.*, 2018; Fossati *et al.*, 2019; Dai *et al.*, 2021; Gawande *et al.*, 2021, 2022). The study of ion channel function of GluD<sub>1R</sub> has been limited since there is no known agonist that binds to GluD<sub>1R</sub> directly to gate opening of the channel. Nonetheless, we and others have demonstrated that GluD<sub>1R</sub> and GluD<sub>2R</sub> carry ionic current upon activation of G $\alpha_q$ -protein-coupled receptors (GqPCRs), either metabotropic glutamate (mGluR, Ady *et al.*, 2013; Dadak *et al.*, 2017; Benamer *et al.*, 2018) or  $\alpha_1$ -adrenergic receptors (Gantz *et al.*, 2020), through a process that involves intact G protein signaling. Intriguingly, in cell lines and brain slices, GluD<sub>1R</sub> and GluD<sub>2R</sub> are open in the presumed absence of agonists and carry tonic cation current (Gantz *et al.*, 2020; Lemoine *et al.*, 2020). The cause of the tonic GluD<sub>1R</sub> current is unknown.

Typically, GPCRs are activated when extracellular ligands bind to the receptor and force a conformational change, which initiates downstream signal transduction mechanisms. In principle, GqPCRs could exhibit low levels of activation in response to ambient ligand, as demonstrated for G $\alpha_{i/o}$ -protein-coupled dopamine D2 receptors (Rodriguez-Contreras *et al.*, 2021). GPCRs can also be constitutively active, entering an active state conformation in the absence of ligand (reviewed in Bond & IJzerman, 2006). Despite knowledge that GluD<sub>1R</sub> is modulated by a GTP-dependent mechanism (Gantz *et al.*, 2020), whether the tonic GluD<sub>1R</sub> current is a product of low-level GqPCR activity is not established.

Here, using patch-clamp electrophysiology in acute mouse brain slices, we show that inverse agonism of  $\alpha_1$ -adrenergic receptors ( $\alpha_1$ -A<sub>R</sub>), which are capable of modulating GluD<sub>1R</sub> current, did not affect tonic GluD<sub>1R</sub> current, indicating that  $\alpha_1$ -A<sub>R</sub> activation was not responsible for generating tonic GluD<sub>1R</sub> current. Further, all methods employed to manipulate G protein activity did not impact the amplitude of the tonic GluD<sub>1R</sub> current. Thus, tonic GluD<sub>1R</sub> current arises from a mechanism separate from ongoing, cell-autonomous GPCR activity. Unlike recent observations with GluD<sub>2R</sub> (Carrillo *et al.*, 2021), we find that GluD<sub>1R</sub> current was not affected by millimolar glycine or D-serine, making it unlikely that tonic GluD<sub>1R</sub> current arises from ambient levels of these amino acids. Instead, both GqPCR-stimulated and tonic GluD<sub>1R</sub> currents were regulated by physiological levels of extracellular calcium. Increasing

extracellular calcium above 2 mM, which is higher than physiological levels but commonly found in artificial cerebral spinal fluids for *in vitro* research (Forsberg *et al*, 2019; Lopes & Cunha, 2019), reduced GluD1<sub>R</sub> unitary current and the magnitude of tonic GluD1<sub>R</sub> by ~50%. When measured at physiological levels of calcium, tonic GluD1<sub>R</sub> current contributes to subthreshold depolarization that drives action potential firing of dorsal raphe neurons.

## Results

### GluD1<sub>R</sub> carries a tonic current

Whole-cell voltage-clamp recordings were made from dorsal raphe neurons in acute brain slices from wild-type mice at 35°C in the presence of GluN, GluA, and GluK receptor blockers, using a potassium-based internal solution ( $V_{\text{hold}} = -65$  mV). Our previous work showed that GluD1<sub>R</sub> carries an ~-20 pA tonic current, revealed by the application of a channel blocker, 1-naphthyl acetyl spermine (NASPM) and by genetic deletion of GluD1<sub>R</sub> (Gantz *et al*, 2020). In agreement with our prior work, here we show that application of NASPM (100  $\mu$ M) produced an apparent outward current of  $17.1 \pm 2.2$  pA (Fig 1A and B). On average, the current peaked in 3.5 min and reversed in 11 min upon washout of NASPM. The outward current was accompanied by an increase in the membrane resistance (Fig 1C) and a reduction in the membrane noise variance ( $\sigma^2$ , Fig 1D), indicating fewer open channels. NASPM failed to change the current when external Na<sup>+</sup> (126 mM) was replaced with N-methyl D-glucamine ( $-3.0 \pm 3.6$  pA,  $P = 0.50$ ,  $n = 3$ ). Voltage ramps from -120 to 10 mV (1 mV/10 ms) before and after application of NASPM showed that tonic GluD1<sub>R</sub> current reversed polarity at ~-2 mV (Fig 1E). In all, these findings reproduce those of our previous work (Gantz *et al*, 2020) and demonstrate that NASPM blocks a tonic, sodium-dependent inward current carried by GluD1<sub>R</sub>.

### Tonic GluD1<sub>R</sub> current is not produced by cell-autonomous G protein activity

GluD1<sub>R</sub> and GluD2<sub>R</sub> carry ionic current following the activation of either mGluR or  $\alpha 1$ -A<sub>R</sub> (Ady *et al*, 2013; Dadak *et al*, 2017; Benamer *et al*, 2018; Gantz *et al*, 2020; Lemoine *et al*, 2020) via a G-protein-dependent mechanism (Dadak *et al*, 2017; Gantz *et al*, 2020). GPCRs can exhibit constitutive activity in the absence of agonist (Prézeau *et al*, 1996), and low-level constitutive activity of GPCRs affects other subthreshold cation conductances (Lu *et al*, 2010; Shen *et al*, 2012; Zhang *et al*, 2012; Quallo *et al*, 2017; Philippart & Khaliq, 2018). But the involvement of GqPCRs in generating tonic GluD1<sub>R</sub> current has not been explored.

To test whether increased G protein activity was sufficient for generating tonic GluD1<sub>R</sub> current, the internal recording solution was supplemented with a non-hydrolyzable GTP analog (guanosine-5'-[( $\beta$ ,  $\gamma$ )-imido]triphosphate, GppNHp, 1 mM), which binds irreversibly to G $\alpha$  and elevates G protein activity. In dorsal raphe neurons, dialysis with GppNHp produces a tonic outward current carried by G protein-coupled inwardly rectifying potassium (GIRK) channels (Loucif *et al*, 2006) by elevating free G $\beta\gamma$  subunits, which gate GIRK channels (Pfaffinger *et al*, 1985). In agreement, whole-cell dialysis

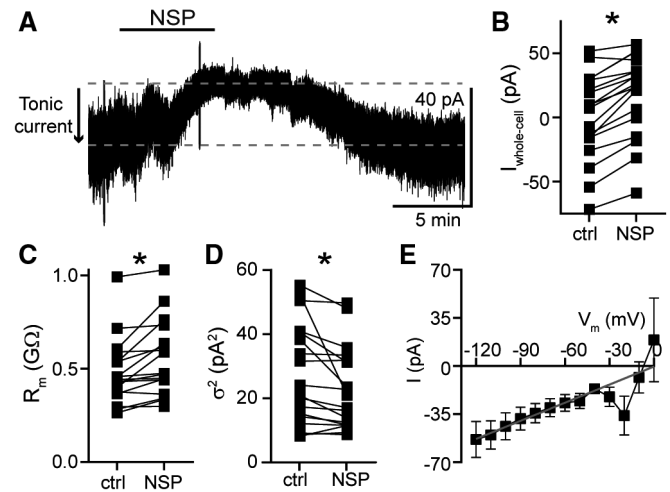


**Figure 1. NASPM reveals a tonic inward current carried by GluD1<sub>R</sub>.**

- A Representative whole-cell voltage-clamp recording of the apparent outward current produced by application of NASPM (NSP, 100  $\mu$ M). Dashed lines indicate baseline current (bottom) and the peak of the outward current (top). Tonic current was measured as the difference of these lines (arrow).
- B Plot of the whole-cell current ( $V_{\text{hold}} = -65$  mV) in control conditions (ctrl) and after application of NASPM (NSP,  $P < 0.0001$ ,  $n = 18$ ).
- C Plot of basal membrane resistance recorded in control conditions (ctrl) and during NASPM application (NSP,  $P = 0.0002$ ,  $n = 17$ ).
- D Plot of membrane noise variance ( $\sigma^2$ ) in control conditions (ctrl) and during NASPM application (NSP,  $P = 0.002$ ,  $n = 18$ ).
- E Current-voltage relationship of the NASPM-sensitive tonic inward current. The linear portion was fit by linear regression (gray line) indicating an  $E_{\text{rev}}$  near 0 mV ( $n = 5$  biological replicates).

Data information: In (B–E), line and error bars represent mean  $\pm$  SEM. In (B–D), \* denotes statistical significance (Wilcoxon matched-pairs signed rank tests).

Source data are available online for this figure.

of GppNHp-containing internal solution ( $\geq 10$  min) produced a tonic outward current with a reversal potential of ~-108 mV (Fig 2A–C), consistent with the expected reversal potential of potassium (calculated  $E_{\text{K}}$ : -104 mV). Application of BaCl<sub>2</sub> (100  $\mu$ M), which blocks GIRK channels (Gantz *et al*, 2013), produced an apparent inward current ( $-46.0 \pm 10.6$  pA, Fig 2A) with GppNHp- but not GTP-containing internal solution (Fig 2C). These data demonstrate that amplifying G protein signaling with GppNHp produces standing currents carried by G protein-gated ion channels, consistent with previous studies (Loucif *et al*, 2006; Kramer & Williams, 2016). In the continued presence of BaCl<sub>2</sub>, tonic GluD1<sub>R</sub> current was measured following application of NASPM (Fig 2D and E). On average, tonic GluD1<sub>R</sub> current was  $-16.7 \pm 2.8$  pA, which was not different from current measured with GTP-containing internal solution (Fig 2D). To determine whether BaCl<sub>2</sub> affected conductance of GluD1<sub>R</sub>, we also examined GluD1<sub>R</sub> current stimulated by synaptic activation of  $\alpha 1$ -A<sub>R</sub> (Gantz *et al*, 2020; Khamma *et al*, 2022). Electrical stimulation of the brain slice (5 pulses, 0.5 ms, 60 Hz) delivered via a monopolar stimulating electrode was used to evoke an  $\alpha 1$ -A<sub>R</sub>-dependent excitatory postsynaptic current ( $\alpha 1$ -A<sub>R</sub>-EPSC), which is carried by GluD1<sub>R</sub> (Gantz *et al*, 2020). External BaCl<sub>2</sub> (100  $\mu$ M) had no effect on the amplitude of

the  $\alpha 1$ -A<sub>R</sub>-EPSC (ctrl:  $-20.6 \pm 3.6$  pA; BaCl<sub>2</sub>:  $-26.0 \pm 4.1$  pA, Fig EV1A–C), indicating that at this concentration, external BaCl<sub>2</sub> does not affect conductance of GluD1<sub>R</sub>. Taken together, the data suggest that augmenting G protein activity has a negligible impact on the amplitude of the tonic current carried by GluD1<sub>R</sub>.

In principle, GPCRs could be activated by ambient ligand in brain slices to produce a small tonic current. In midbrain dopamine neurons, ambient activation of G $\alpha_{i/o}$ -coupled dopamine D2 receptors produces a tonic GIRK current of  $\sim 9$  pA (Rodríguez-Contreras et al, 2021). Next, we tested whether tonic GluD1<sub>R</sub> current was dependent on  $\alpha 1$ -A<sub>R</sub> activity, either from ambient ligand or

constitutive activity, by applying an  $\alpha 1$ -A<sub>R</sub> inverse agonist prazosin (100 nM, Hein et al, 2001). Prazosin had no effect on the magnitude of the tonic GluD1<sub>R</sub> current ( $-19.9 \pm 2.8$  pA, Fig EV2A and B). In midbrain dopamine neurons, GluD1<sub>R</sub> current is produced by activation of mGluR (Benamer et al, 2018), suggesting that a similar mechanism may occur in the dorsal raphe. Moreover, in the dorsal raphe, G $\alpha_q$ -coupled histamine H<sub>1</sub> and orexin OX<sub>2</sub> receptors converge on the same downstream effectors as  $\alpha 1$ -A<sub>R</sub> (Brown et al, 2002), suggesting that if tonic GluD1<sub>R</sub> current was produced via G protein activity, there are many types of receptors to consider. As a broad test as to whether tonic GluD1<sub>R</sub> current was dependent on G protein signaling, recordings were made with an internal solution where GTP was replaced with a non-hydrolyzable analog of GDP, GDP $\beta$ S-Li<sub>3</sub> (1.24 mM), which acts as a competitive antagonist at GTP-binding sites and arrests G protein signaling. Within 10 min of whole-cell dialysis with GDP $\beta$ S-containing internal solution, application of noradrenaline (30  $\mu$ M) produced an inward GluD1<sub>R</sub> current (Fig 3A and B). By  $\geq 20$  min of whole-cell dialysis, the noradrenaline-induced current was abolished (Fig 3A and B), confirming efficacy of GDP $\beta$ S to arrest  $\alpha 1$ -A<sub>R</sub>-GluD1<sub>R</sub> signaling (Gantz et al, 2020). In contrast, GDP $\beta$ S had no effect on tonic GluD1<sub>R</sub> current when compared with GTP-containing internal solution with or without a similar concentration of LiCl (GDP $\beta$ S-Li<sub>3</sub>:  $-28.7 \pm 4.9$  pA,  $n = 13$ , GTP:  $-19.3 \pm 2.7$  pA, GTP + LiCl:  $-23.5 \pm 3.9$  pA, Fig 3C). Further, there was no decrement in the magnitude of tonic GluD1<sub>R</sub> current with repeat applications of NASPM (Fig 3D and E). These results demonstrate that tonic GluD1<sub>R</sub> current is independent of cell-autonomous G protein signaling.

Collectively we have shown, using pharmacological and genetics strategies, that GluD1<sub>R</sub> carries ionic current that can be observed in two ways: either by activating  $\alpha 1$ -A<sub>R</sub>, which augments GluD1<sub>R</sub> current in a G-protein-dependent manner, or by measuring tonic GluD1<sub>R</sub> current that arises from a G-protein-independent mechanism. These features distinguish GluD1<sub>R</sub> current from sodium current carried by sodium leak NALCN channels. NALCN current is stimulated by GqPCR activation in a G-protein-independent manner (Lu et al, 2009), whereas “tonic” NALCN current is G-protein-dependent (Lu et al, 2010; Philippart & Khaliq, 2018; reviewed in Ren, 2011). Nonetheless, sufficient similarity between the conductances warrants closer examination of the pharmacological tools used on these channels. The trivalent ion gadolinium (Gd<sup>3+</sup>) effectively blocks NALCN channels, with  $> 80\%$  reduction in NALCN current with 10  $\mu$ M Gd<sup>3+</sup> (Lu et al, 2007, 2009, 2010; Chua et al, 2020). Here, Gd<sup>3+</sup> (10  $\mu$ M) had no significant effect on the amplitude of the  $\alpha 1$ -A<sub>R</sub>-EPSC (Fig EV3A–C) nor on the magnitude of the tonic NASPM-sensitive current (Fig EV3D and E).

### Tonic GluD1<sub>R</sub> current is not augmented by glycine or D-serine

Using clusters of HEK-293T cells and synaptically connected cultured cerebellar neurons, Carrillo et al (2021) demonstrate that GluD2<sub>R</sub> can be opened by external glycine or D-serine with an EC<sub>50</sub> of  $\sim 1$  and 3 mM respectively and produce a steady-state current. Previously, we demonstrated that high concentrations (10 mM) of glycine and D-serine reduce the  $\alpha 1$ -A<sub>R</sub>-EPSC without affecting unitary channel current (Gantz et al, 2020); attributing the diminished current to glycine inducing a desensitized state of the channel (Hansen et al, 2009). When applied at 1 mM, neither glycine (in the

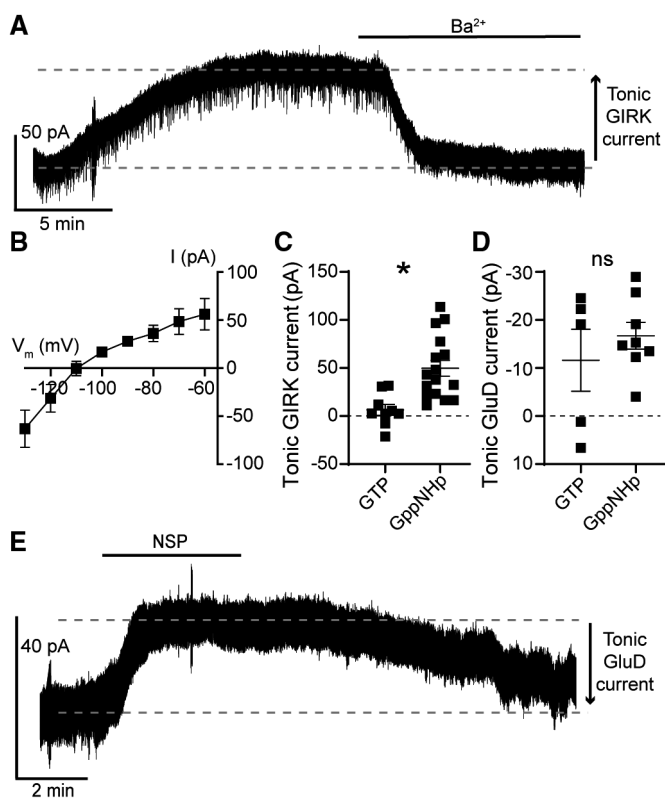


**Figure 2. Augmentation of G protein activity with GppNHp has no effect on tonic GluD1<sub>R</sub> current.**

- A GppNHp-containing internal solution produced a tonic Ba<sup>2+</sup>-sensitive (100  $\mu$ M) outward current carried by GIRK channels, shown in a representative whole-cell voltage-clamp recording.
- B Current–voltage relationship of the tonic Ba<sup>2+</sup>-sensitive (100  $\mu$ M) outward GIRK current demonstrating reversal near expected E<sub>K</sub> and inward rectification ( $n = 6$  biological replicates).
- C Plot of tonic GIRK currents measured in control conditions (GTP) and with GppNHp-containing internal solution ( $P = 0.0003$ ,  $n = 9$  and 16 biological replicates respectively).
- D Plot of the magnitude of tonic GluD1<sub>R</sub> current measured with GTP-containing internal solution as compared to GppNHp-containing internal solution ( $P = 0.72$ ,  $n = 5$  and 8 biological replicates respectively) when measured in external Ba<sup>2+</sup> to block tonic GIRK current.
- E GppNHp had no effect on the NASPM (NSP, 100  $\mu$ M)-sensitive inward current, shown in a representative trace.

Data information: In (B–D), line and error bars represent mean  $\pm$  SEM.

\* denotes statistical significance, ns denotes not significant (Mann–Whitney tests).

Source data are available online for this figure.

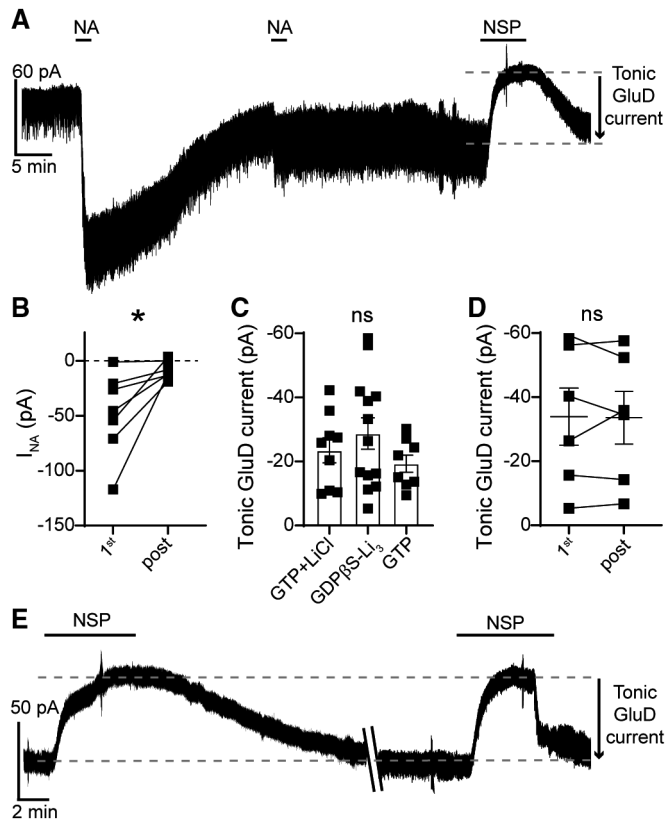


**Figure 3. Tonic GluD<sub>1R</sub> current is not dependent on G protein signaling.**

- A With GDPβS-containing internal solution, noradrenaline-induced GluD<sub>1R</sub> current ( $I_{NA}$ ) was diminished by > 20 min post-dialysis, shown in a representative trace.
- B With GDPβS-containing internal solution, the amplitude of  $I_{NA}$  ran down with whole-cell dialysis; shown in a plot of the first application of noradrenaline (30  $\mu$ M, 1<sup>st</sup>) compared to application of noradrenaline > 20 min post-dialysis (post,  $P = 0.02$ ,  $n = 7$ ).
- C Plot of the magnitude of tonic GluD<sub>1R</sub> current measured after dialysis with GTP<sup>+</sup>LiCl<sup>-</sup>, GDPβS-Li<sub>3</sub><sup>-</sup>, and GTP-containing internal solution, displaying no significant difference between the groups ( $P = 0.46$ ,  $n = 9, 13, 8$  biological replicates respectively).
- D Plot of the magnitude of tonic GluD<sub>1R</sub> current recorded with GDPβS-containing internal solution for the first application of NASPM (1<sup>st</sup>) and application of NASPM > 45 min post-dialysis, showing no difference in the average amplitude (post,  $P = 0.84$ ,  $n = 6$  biological replicates).
- E With GDPβS-containing internal solution, repeated application of NASPM revealed tonic GluD<sub>1R</sub> current without a decrement in amplitude, shown in a representative trace. \ indicate a 40-min wash in the recording.

Data information: In (B–D), line and error bars represent mean  $\pm$  SEM. \* denotes statistical significance, ns denotes not significant (B and D: Wilcoxon matched-pairs signed rank tests; C: Kruskal–Wallis test). Source data are available online for this figure.

presence of 10  $\mu$ M strychnine) nor D-serine affected the  $\alpha$ 1-A<sub>R</sub>-EPSC (Fig 4A–E). Neither glycine nor D-serine produced a change in whole-cell current (Fig 4E–G) or membrane resistance (glycine:  $P = 0.72$ ,  $n = 15$ ; D-serine:  $P = 0.09$ ,  $n = 12$ ). Lastly, the magnitude of tonic GluD<sub>1R</sub> current was measured by application of NASPM (100  $\mu$ M) in the presence of glycine or D-serine (1 mM). Tonic GluD<sub>1R</sub> current was not changed by either amino acid at this concentration (Fig 4H).

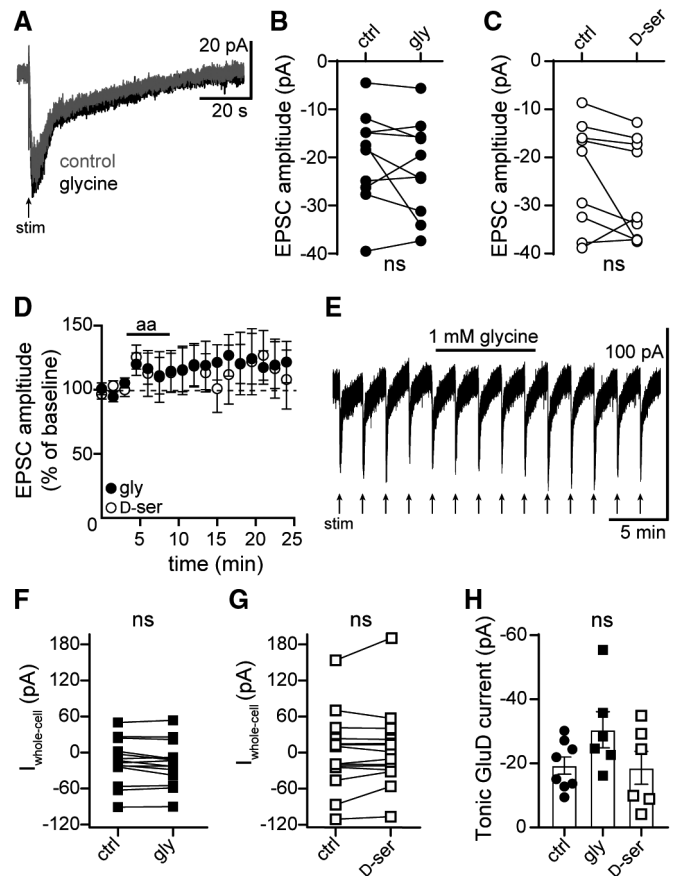


**Figure 4. Tonic GluD<sub>1R</sub> current is not produced by external glycine or D-serine.**

- A Representative traces of electrically evoked (arrow)  $\alpha$ 1-A<sub>R</sub>-EPSCs in control conditions and after application of glycine (1 mM).
- B, C Plot of the amplitude of the  $\alpha$ 1-A<sub>R</sub>-EPSC in control conditions (ctrl) and in glycine (1 mM,  $P = 0.43$ ,  $n = 10$  biological replicates, B), or D-serine (1 mM,  $P = 0.13$ ,  $n = 9$  biological replicates, C).
- D Glycine or D-serine (aa) had no significant effect on the amplitude of the  $\alpha$ 1-A<sub>R</sub>-EPSC, shown in a time-course plot ( $n = 10$  and 9 biological replicates for glycine and D-serine respectively).
- E Glycine had no significant effect on the amplitude of the  $\alpha$ 1-A<sub>R</sub>-EPSC (arrow) or whole-cell current, shown in a representative trace.
- F, G Plot of the whole-cell current in control conditions (ctrl) and in glycine ( $P = 0.39$ ,  $n = 14$  biological replicates, F) or D-serine ( $P = 0.54$ ,  $n = 14$  biological replicates, G).
- H Plot of the magnitude of tonic GluD<sub>1R</sub> current measured in control conditions (ctrl), or in the presence of glycine (gly) or D-serine (D-ser), showing no difference in the amplitude of tonic GluD<sub>1R</sub> current ( $P = 0.20$ ,  $n = 8, 6, 6$  biological replicates respectively).

Data information: In (B–D and F–H), line and error bars represent mean  $\pm$  SEM. ns denotes not significant (B, C and F, G: Wilcoxon matched-pairs signed rank tests; H: Kruskal–Wallis test). Source data are available online for this figure.

One possibility is that glycine and D-serine do not directly gate GluD<sub>1R</sub>, as observed for GluD<sub>2R</sub> (Carrillo *et al*, 2021). Alternatively, if tonic GluD<sub>1R</sub> current is produced by ambient levels of glycine or D-serine, the channels may be open in a desensitized low-conductance state, akin to steady-state current produced by conducting desensitized GluA<sub>R</sub> (Coombs *et al*, 2019). In

constitutively open mutant GluD<sub>2R</sub>, desensitization by D-serine is reduced dramatically by high levels of extracellular calcium (> 3 mM) through a mechanism that involves calcium binding and stabilization of the ligand-binding domain dimer interface (Hansen et al, 2009). Therefore, we increased the concentration of calcium in the extracellular solution to 4.8 mM and then applied glycine (1 mM). In 4.8 mM calcium, glycine (in the presence of 10 μM strychnine) had no effect on the α1-A<sub>R</sub>-EPSC (99.2 ± 5.5% of the amplitude in glycine) or whole-cell current (−0.42 ± 2.6 pA change in glycine, *P* = 0.84 for both comparisons, *n* = 6, Wilcoxon matched-pairs signed rank tests). Together these results suggest that GluD<sub>1R</sub> current is not affected by millimolar glycine or D-serine. Further it is unlikely that tonic GluD<sub>1R</sub> current arises from ambient levels of glycine or D-serine.

### Tonic GluD<sub>1R</sub> current is reduced by elevated extracellular calcium

To further examine whether tonic GluD<sub>1R</sub> current is a product of desensitized low-conductance channels, we characterized the effect of increasing the concentration of extracellular calcium. Increasing extracellular calcium from physiological 1.2 mM (Forsberg et al, 2019, our standard recording solution) to 2.4 mM had no significant effect on the amplitude of the α1-A<sub>R</sub>-EPSC (*P* = 0.18, *n* = 18, Fig 5A), the time-to-peak (*P* = 0.22, *n* = 14), or the rate of decay (*P* = 0.17, *n* = 14, Wilcoxon matched-pairs signed rank tests). However, increasing extracellular calcium to 4.8 mM rapidly reduced the α1-A<sub>R</sub>-EPSC by ~40% (Fig 5A and B) accompanied by a significant slowing in the rate of decay (Fig 5B and C). Typically, the α1-A<sub>R</sub>-EPSC peaks in ~1 s from stimulation (Khamma et al, 2022) and decays by ~50% by 5 s from stimulation (Fig EV4A and B). In 4.8 mM calcium, the α1-A<sub>R</sub>-EPSC persisted with no significant decrement in amplitude for 5 s from stimulation (Fig EV4B). In 1.2 mM calcium, the α1-A<sub>R</sub>-EPSC membrane noise variance (σ<sup>2</sup>)–amplitude relationship was fit well by linear regression, yielding an estimate of a −1.04 pA unitary current (Fig 5D), consistent with our previous report (Gantz et al, 2020). In 2.4 mM calcium, there was a significant decrease in the slope of the α1-A<sub>R</sub>-EPSC σ<sup>2</sup>–amplitude relationship (*P* = 0.044, *n* = 73 and 20, simple linear regression) yielding an estimate of a −0.54 pA unitary current (Fig 5D). In 4.8 mM calcium, there was no longer a relationship between the α1-A<sub>R</sub>-EPSC membrane noise variance (σ<sup>2</sup>) and amplitude (Fig 5D). Thus, elevating extracellular calcium reduces but prolongs the time course of α1-A<sub>R</sub>-stimulated GluD<sub>1R</sub> current.

Next, we assessed the magnitude of the tonic GluD<sub>1R</sub> current. On average, the tonic GluD<sub>1R</sub> current was −9.0 and −7.5 pA in 2.4 and 4.8 mM calcium, respectively (Fig 5E and F). When compared with measurements in 1.2 mM calcium, elevating extracellular calcium caused significant reductions in the magnitude of tonic GluD<sub>1R</sub> current (Fig 5F). To determine whether GluD<sub>1R</sub> current was reduced by resting levels of extracellular calcium, we measured tonic GluD<sub>1R</sub> current in nominally calcium-free external solution. Following the elimination of the α1-A<sub>R</sub>-EPSC, which served as a control for the removal of extracellular calcium (Gantz et al, 2020), NASPM was applied. On average, the magnitude of the tonic GluD<sub>1R</sub> current in nominally calcium-free solution was larger, ~30 pA (Fig 5G and H). The magnitude of the tonic GluD<sub>1R</sub> current measured in

nominally calcium-free solution was not changed significantly by the addition of the Gd<sup>3+</sup> (10 μM, Fig EV3F).

In our prior work, we demonstrated that the GluD<sub>1Rs</sub> that underlie the α1-A<sub>R</sub>-EPSC are at least transiently open at rest since the channel pores were accessible to the open-channel blocker NASPM in the absence of α1-A<sub>R</sub> stimulation (Koike et al, 1997; Gantz et al, 2020). To determine whether the loss of GluD<sub>1R</sub> current in elevated extracellular calcium reflects a change in gating of GluD<sub>1R</sub>, we tested whether increasing extracellular calcium affected the block of the α1-A<sub>R</sub>-EPSC by NASPM. Consistent with our prior work (Gantz et al, 2020), when applied in 1.2 mM calcium, NASPM (100 μM, 6 min) blocked the α1-A<sub>R</sub>-EPSC (93.3 ± 1.6% reduction, Fig 5I). In 2.4 mM calcium, NASPM blocked the α1-A<sub>R</sub>-EPSC to a similar degree (92.9 ± 2.0% reduction, Fig 5I). In 4.8 mM calcium, NASPM blocked α1-A<sub>R</sub>-EPSC, but to a lesser degree (80.9 ± 3.5% reduction, Fig 5I). These data indicate that in 4.8 mM calcium, GluD<sub>1R</sub> are less accessible to open-channel block by NASPM. In GluN<sub>R</sub>, pore block by magnesium prevents binding of the open-channel blocker MK-801 (Reynolds & Miller, 1988; Hubbard et al, 1989). Since both magnesium and MK-801 block the pore and eliminate GluN<sub>R</sub> current, the “protection” provided by magnesium is apparent in the rate of recovery of the GluN<sub>R</sub> current upon washout and dissociation of MK-801 (McKay et al, 2013). Therefore, we examined the rate of recovery of the α1-A<sub>R</sub>-EPSC upon washout of NASPM. NASPM was applied in either 1.2 or 4.8 mM calcium, then NASPM was washed out and the α1-A<sub>R</sub>-EPSC recovered in 1.2 mM calcium (Fig 5J and K). After 12 min of wash, the α1-A<sub>R</sub>-EPSC blocked by NASPM in 4.8 mM calcium had fully recovered (105 ± 3.5%), whereas the α1-A<sub>R</sub>-EPSC blocked by NASPM in 1.2 mM calcium had only partially recovered (49.9 ± 10.0%, Fig 5K). Therefore, high levels of extracellular calcium inhibit GluD<sub>1R</sub> in a way that antagonizes open-channel block by NASPM. Taken together, the data suggest that extracellular calcium has direct inhibitory action on GluD<sub>1R</sub> current.

### Tonic GluD<sub>1R</sub> current provides subthreshold drive of action potential firing

*In vivo* and *in vitro*, dorsal raphe neurons fire action potentials (APs) in a rhythmic “pacemaker” manner. Primarily, serotonin neurons are not autonomous pacemakers, but require subthreshold drive from noradrenergic afferents and activation of α1-A<sub>R</sub> (Baraban et al, 1978). In the absence of noradrenaline, dorsal raphe neurons are silent or fire slowly and erratically (Svensson et al, 1975; Baraban et al, 1978). To determine if tonic GluD<sub>1R</sub> current contributed to subthreshold excitation, whole-cell current clamp recordings were made from dorsal raphe neurons, and APs were evoked with somatic current injection (1.5 s, 20 pA increments, Fig 6A). Consistent with the absence of ambient noradrenaline in brain slices (Gantz et al, 2020), 5/10 neurons were firing spontaneously at a slow and irregular rate (0.8 ± 0.3 Hz); but all fired in response to current injection. After application of NASPM (30–50 μM), 1/10 neurons fired spontaneously, and the rest became quiescent (silent) until APs were evoked by current injection (Fig 6B). At subthreshold potentials (−80 to −55 mV), NASPM hyperpolarized the membrane by ~7–10 mV (Fig 6C), consistent with Ohm’s law given the magnitude of the tonic GluD<sub>1R</sub> current (−17.1 ± 2.2 pA) and basal membrane resistance (481.1 ± 43.2 MΩ). Consequently, NASPM increased the minimum current necessary to evoke AP firing

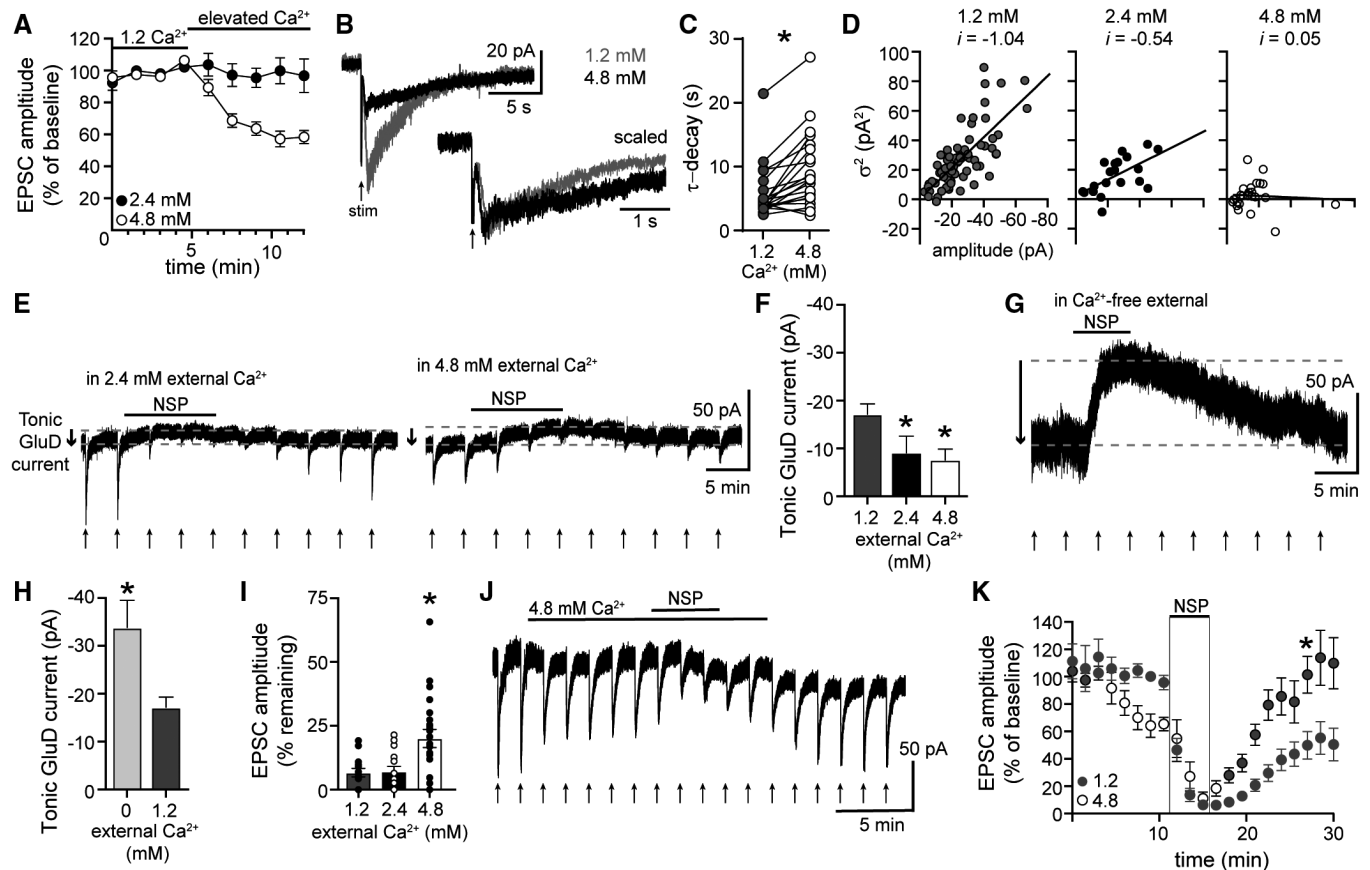


**Figure 5. GluD<sub>1R</sub> current is inhibited by extracellular calcium.**

- A Increasing extracellular calcium to 4.8 mM reduced the amplitude of the  $\alpha 1$ -A<sub>R</sub>-EPSC, shown in a time-course plot ( $n = 18$  and 26 biological replicates for 2.4 and 4.8 mM respectively).
- B Representative traces of electrically evoked (arrow)  $\alpha 1$ -A<sub>R</sub>-EPSCs in control conditions (1.2 mM calcium) and after application of 4.8 mM calcium. Lower right inset shows the same traces scaled to their peak to illustrate the increase in rate of decay in 4.8 mM calcium.
- C Plot of the rate of decay of the  $\alpha 1$ -A<sub>R</sub>-EPSC in control conditions (1.2 mM) and in 4.8 mM extracellular calcium ( $P < 0.0001$ ,  $n = 21$  biological replicates).
- D Plots of the  $\alpha 1$ -A<sub>R</sub>-EPSC variance versus mean amplitude in control conditions (1.2 mM), 2.4 mM, and 4.8 mM extracellular calcium, linear fits represent mean unitary current ( $i$ , 1.2 mM:  $r^2 = 0.53$ ,  $P < 0.0001$ ,  $n = 73$ ; 2.4 mM:  $r^2 = 0.36$ ,  $P = 0.006$ ,  $n = 20$ ; 4.8 mM:  $r^2 = 0.004$ ,  $P = 0.748$ ,  $n = 26$  biological replicates).
- E Elevating extracellular calcium to 2.4 and 4.8 mM decreased the response to NASPM (NSP), shown in representative traces. Arrows indicate time of electrical stimulation and resulting  $\alpha 1$ -A<sub>R</sub>-EPSCs.
- F Plot of the magnitude of tonic GluD<sub>1R</sub> current measured by application of NASPM in control conditions (1.2 mM), 2.4 and 4.8 mM calcium. The magnitude of tonic GluD<sub>1R</sub> current in 2.4 and 4.8 mM calcium was reduced relative to control conditions (1.2 mM:  $n = 18$ ; 2.4 mM:  $P = 0.03$ ,  $n = 17$ ; 4.8 mM:  $P = 0.005$ ,  $n = 22$  biological replicates).
- G In nominally calcium-free external, NASPM produced a large apparent outward current, shown in a representative whole-cell voltage-clamp recording. Arrows indicate time of electrical stimulation and absence of  $\alpha 1$ -A<sub>R</sub>-EPSCs.
- H Plot of the magnitude of tonic GluD<sub>1R</sub> current measured by application of NASPM in control conditions (1.2 mM) and nominally calcium-free (0) solution. The magnitude of tonic GluD<sub>1R</sub> current in calcium-free was larger than control conditions ( $P = 0.009$ ,  $n = 18$  and 14 biological replicates).
- I Plot of the inhibition of the  $\alpha 1$ -A<sub>R</sub>-EPSC by application of NASPM in control conditions (1.2 mM), 2.4 mM, and 4.8 mM extracellular calcium (1.2 vs. 2.4 mM:  $P > 0.999$ , 1.2 vs. 4.8 mM:  $P = 0.026$ ,  $n = 14$ , 15, and 22 biological replicates).
- J Elevating extracellular calcium to 4.8 mM reduces the change in whole-cell current to NASPM and accelerates recovery of the  $\alpha 1$ -A<sub>R</sub>-EPSC from NASPM-block in control conditions (1.2 mM extracellular calcium), shown in a representative whole-cell voltage-clamp recording.
- K Time course of the block and recovery of the  $\alpha 1$ -A<sub>R</sub>-EPSC by application of NASPM when applied in 4.8 mM extracellular calcium but allowed to recover in control conditions (1.2 mM), shown in comparison with the time course of the block and recovery of the  $\alpha 1$ -A<sub>R</sub>-EPSC by application of NASPM when applied in control conditions (1.2 mM extracellular, as shown in C). Gray fill circles indicate measurements made in 1.2 mM, whereas open circles indicate measurements made in 4.8 mM extracellular calcium ( $P = 0.0007$ , 1.2:  $n = 7$ –14, 4.8:  $n = 6$ –7 biological replicates).

Data information: In (A, F, H, I, K), line and error bars represent mean  $\pm$  SEM. \* denotes statistical significance, ns denotes not significant (C: Wilcoxon matched-pairs signed rank test; D: Simple linear regression; F and I: Kruskal–Wallis tests; H and K: Mann–Whitney tests).

Source data are available online for this figure.

(approximate rheobase), which reversed upon 10 min washout of NASPM (Fig 6D) and increased the latency to fire the first AP (Fig 6E). In contrast, once the membrane reached threshold,

NASPM had little-to-no effect on average membrane potential between APs (Fig 6C). Further, the AP waveform was unaffected by NASPM (Fig 6F). There were no differences in the AP half-width

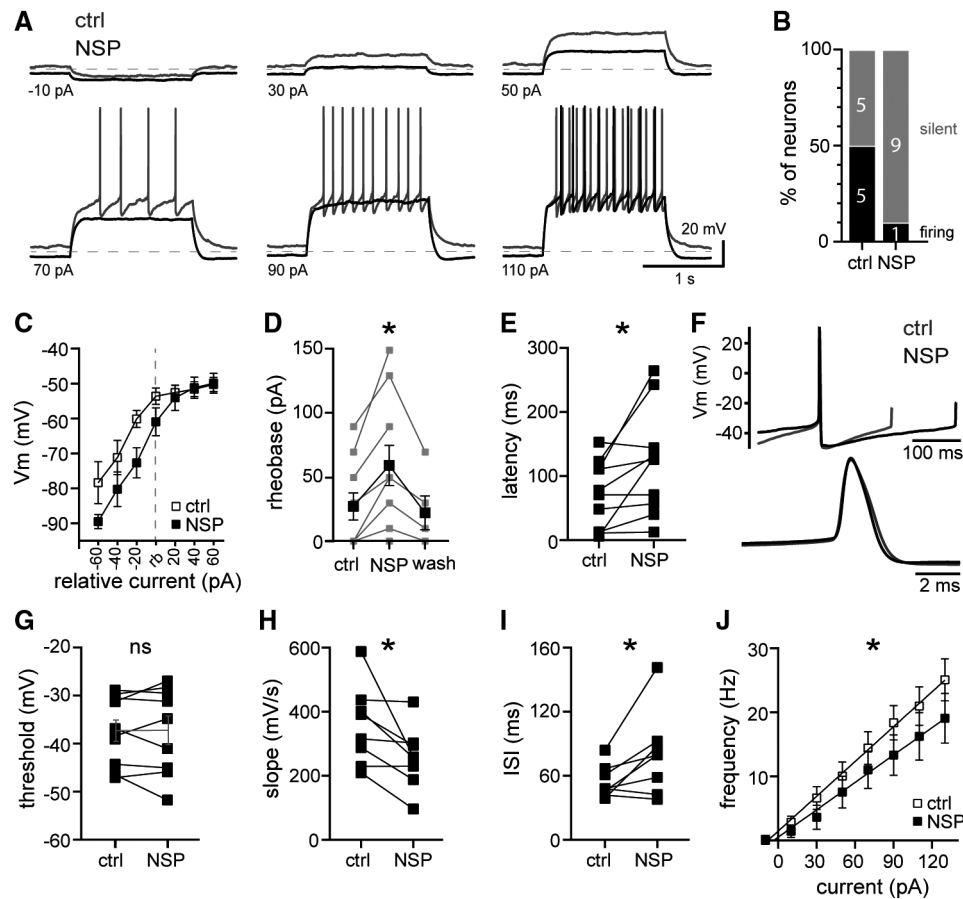


**Figure 6. Tonic GluD1<sub>R</sub> current provides subthreshold drive of action potential firing.**

- A Representative traces of whole-cell current clamp recordings of membrane potential and AP firing evoked by current injection (1.5 s) demonstrating hyperpolarization by NASPM. Dashed line is at  $-80$  mV.
- B Distribution of firing response in control (ctrl) and after application of NASPM (NSP). In control conditions 5/10 neurons fired spontaneously without current injection and 5/10 were silent. In the same neurons after NASPM, 1/10 fired spontaneously and 9/10 were silent.
- C Plot of the membrane potential ( $V_m$ ) versus injected current relative to rheobase (rb) in control and NASPM, demonstrating that NASPM produced a hyperpolarization at subthreshold potentials ( $n = 10$  biological replicates).
- D Plot of the minimum current needed to induce firing (approximate rheobase) in control conditions, NASPM, and following wash out of NASPM (10 min;  $P = 0.005$ ,  $n = 5$ –10 biological replicates).
- E NASPM increased the latency to fire the first AP upon current injection (150 pA,  $P = 0.01$ ,  $n = 10$  biological replicates).
- F Average AP waveform recorded in control and in NASPM, aligned at peaks. Below, expanded timescale.
- G NASPM had no effect on the AP threshold (150 pA, measured from the 2<sup>nd</sup> AP,  $P < 0.99$ ,  $n = 9$  biological replicates).
- H NASPM decreased the slope of the voltage trajectory between APs (90 pA, measured in the middle 60% of the interspike interval of the first five APs,  $P = 0.02$ ,  $n = 8$  biological replicates).
- I NASPM increased the interspike interval during evoked firing (90 pA, averaged from first five APs,  $P = 0.04$ ,  $n = 8$  biological replicates).
- J Plot of the initial firing frequency (first three APs) versus injected current in control and NASPM ( $P = 0.01$ ,  $n = 10$  biological replicates).

Data information: In (C–E and G–J), line and error bars represent mean  $\pm$  SEM. ns denotes not significant (D: one-way mixed effects ANOVA, E and G–I: Wilcoxon matched-pairs signed rank tests; J: two-way ANOVA).

Source data are available online for this figure.

( $P = 0.19$ ), after-hyperpolarization ( $P = 0.38$ ), height ( $P = 0.06$ ), or threshold (Fig 6G). But there was a significant decrease in the slope of the voltage trajectory between APs (Fig 6F and H), resulting in a delay to the next AP (interspike interval, Fig 6I). Overall, NASPM reduced AP firing frequency (measured from the first three APs, Fig 6J). Thus, at physiological levels of extracellular calcium, tonic GluD1<sub>R</sub> current contributes to subthreshold drive of action potential firing.

## Discussion

### Ion channel function of GluD1 receptors

GluD1<sub>R</sub> and GluD2<sub>R</sub> carry ionic current following the activation of either mGluR or  $\alpha 1$ -A<sub>R</sub> (Ady et al, 2013; Dadak et al, 2017; Benamer et al, 2018; Gantz et al, 2020; Lemoine et al, 2020). GluD2<sub>R</sub> current, seen upon mGluR1 activation in cell lines, is dependent on

canonical GqPCR signaling as the agonist-induced current is blocked by bath application of  $G\alpha_q$  or phospholipase C inhibitors (Dadak *et al*, 2017). Similarly, GluD1<sub>R</sub> ionic current activated by  $\alpha 1$ -A<sub>R</sub> in dorsal raphe neurons is abolished after internal dialysis with GDP $\beta$ S-Li<sub>3</sub> (Gantz *et al*, 2020), a nonspecific disruptor of G protein activity and other processes requiring a GDP-GTP exchange, demonstrating a cell-autonomous requirement of intact G protein signaling. Following our original report of tonic GluD1<sub>R</sub> current in brain slices (Gantz *et al*, 2020), Lemoine *et al* (2020) reported a similar tonic current carried by GluD2<sub>R</sub> when expressed in cell lines with mGluR1. mGluR, like many GPCRs, can exhibit constitutive activity in the absence of agonist (Prézeau *et al*, 1996), and low-level constitutive activity of GPCRs affects other subthreshold cation conductances (Lu *et al*, 2010; Shen *et al*, 2012; Zhang *et al*, 2012; Quallo *et al*, 2017; Philippart & Khaliq, 2018). Here we show that tonic GluD1<sub>R</sub> current is not produced by low-level, cell-autonomous activation of GPCRs. Augmentation of ongoing G protein activity amplified tonic potassium current carried by GIRK channels, but not tonic GluD1<sub>R</sub> current. Further, depletion of cell-autonomous G protein activity did not change the amplitude of the tonic GluD1<sub>R</sub> current. Thus, tonic GluD1<sub>R</sub> current arises from a mechanism separate from ongoing GPCR activity.

In addition to modulation by GPCRs, GluD1<sub>R</sub> and GluD2<sub>R</sub> are regulated by external glycine and D-serine. These amino acids are known to inhibit constitutively active mutant GluD1<sub>R</sub> and GluD2<sub>R</sub> “Lurcher” channels (Naur *et al*, 2007; Yadav *et al*, 2011) and GPCR-stimulated GluD1<sub>R</sub> and GluD2<sub>R</sub> currents (Ady *et al*, 2013; Benamer *et al*, 2018; Gantz *et al*, 2020). However, D-serine converts from an inhibitor to an agonist of GluD2<sub>R</sub> Lurcher channels, when the dimer interface is stabilized while reducing conformational constraints in the ligand-binding domain (Hansen *et al*, 2009). Glycine and D-serine can also open wild-type GluD2<sub>R</sub> in HEK-293T cell clusters or synaptically coupled cultured cerebellar neurons through a gating mechanism that requires binding of the N-terminal domains to pre-synaptic scaffold proteins or otherwise constraining movement in the N-terminal domains with cysteine-cross-linking (Carrillo *et al*, 2021). In contrast, we find that GluD1<sub>R</sub> current was unaffected by millimolar glycine or D-serine. Neither amino acid produced a significant inward current nor affected the magnitude of the  $\alpha 1$ -A<sub>R</sub>-stimulated GluD1<sub>R</sub> current or tonic GluD1<sub>R</sub> current. Therefore, it may be that glycine and D-serine do not directly gate GluD1<sub>R</sub>, as observed for GluD2<sub>R</sub> (Carrillo *et al*, 2021); yet another unidentified endogenous ligand for GluD1<sub>R</sub> cannot be ruled out. Alternatively, tonic GluD1<sub>R</sub> current may be a product of a low conductance state of GluD1<sub>R</sub>, akin to “steady-state” current produced by conducting desensitized GluA<sub>R</sub> (Coombs *et al*, 2019). If tonic GluD1<sub>R</sub> current is a product of desensitized low-conductance GluD1<sub>R</sub>, then conditions that prevent desensitization (e.g., increasing extracellular calcium, Hansen *et al*, 2009) may paradoxically reduce GluD1<sub>R</sub> current. Indeed, we found that  $\alpha 1$ -A<sub>R</sub>-stimulated and tonic GluD1<sub>R</sub> currents were bidirectionally regulated by extracellular calcium: increasing extracellular calcium reduced GluD1<sub>R</sub> current and decreasing extracellular calcium augmented GluD1<sub>R</sub> current. In addition, increasing extracellular calcium slowed the decay rate of the  $\alpha 1$ -A<sub>R</sub>-stimulated GluD1<sub>R</sub> current, which may reflect slowing of channel desensitization. High levels of extracellular calcium also “protected” GluD1<sub>R</sub> from open-channel block by NASPM. Thus, extracellular calcium has direct inhibitory action on native GluD1<sub>R</sub> current in brain slices,

either by reducing open channel probability or directly blocking the channel. Future work is needed to distinguish between these possibilities, and it is important to note that several mechanisms may be at play since extracellular calcium is known to affect GluN<sub>R</sub> gating through multiple binding sites (Maki & Popescu, 2014).

### Importance of tonic cation conductances in excitability

Throughout the central nervous system, many types of neurons fire action potentials in a rhythmic “pacemaker” pattern. Some are autonomous pacemakers, driven by intrinsic membrane properties, while others are conditional pacemakers that rely on synaptic input and receptor stimulation. A common feature in autonomous pacemakers is the presence of a tonic, subthreshold, tetrodotoxin-insensitive, cation/sodium current (Raman *et al*, 2000; Jackson *et al*, 2004; Lu *et al*, 2007; Khaliq & Bean, 2010; Eggermann *et al*, 2011; Li *et al*, 2021). While many different types of channels are involved, these tonic currents each function to depolarize the membrane to  $\sim -60$  mV where voltage-dependent mechanisms of action potential firing are engaged. Primarily, serotonin neurons are conditional pacemakers and require subthreshold drive from noradrenergic afferents and activation of  $\alpha 1$ -A<sub>R</sub> (Baraban *et al*, 1978; Vandermaelen & Aghajanian, 1983) much like other conditional pacemakers, which require activation of  $G\alpha_q$ -coupled orexin or muscarine receptors (Egorov *et al*, 2002, 2019; van den Top *et al*, 2004; Yamada-Hanff & Bean, 2013). In these neurons, activation of GqPCRs leads to subthreshold ( $\sim -70$  to  $-55$  mV) depolarization via a very similar cation current as the tonic current observed in autonomous pacemakers. While these tonic cation currents are essential for subthreshold depolarization, it is not unusual for the current to be quite small, only a few to tens of picoamperes (Raman *et al*, 2000; Taddese & Bean, 2002; Jackson *et al*, 2004).

Here we show that GluD1<sub>R</sub> carried tonic cation current of  $\sim -17$  pA at subthreshold potentials ( $-80$  to  $-55$  mV), which depolarized the membrane by  $\sim 7$  mV. Block of tonic GluD1<sub>R</sub> current silenced a subset of dorsal raphe neurons that were firing spontaneously in the brain slice. Under conditions of GluD1<sub>R</sub> channel block, dorsal raphe neurons required more somatic current injection to fire. Block of tonic GluD1<sub>R</sub> current had little effect on the shape of the APs but prolonged the interval between APs, consistent with a reversal potential of  $\sim 0$  mV and intrinsic inward rectification (Gantz *et al*, 2020). However, it should be noted that NASPM preferentially blocks inward flow, and strong depolarization relieves pore block (Koike *et al*, 1997). Thus, observation of any contribution of outward ion flux may be obscured. It is worth noting that tonic or steady-state current is not an unusual feature of GluD1<sub>R</sub>. Long-lasting synaptic currents and tonic currents are observed by the other members of the iGluR family: GluN<sub>R</sub> (Sah *et al*, 1989; Misra *et al*, 2000; Meur *et al*, 2007; Chiu & Jahr, 2017; Hanson *et al*, 2019), kainate<sub>R</sub> (Castillo *et al*, 1997), and GluA<sub>R</sub> either when recovering from desensitization in continued presence of glutamate (Lu *et al*, 2017) or when conducting while desensitized (Coombs *et al*, 2019). Further, desensitization-resistant GluA<sub>R</sub> carries a long-lasting “pedestal” current in CA1 pyramidal neurons, which powerfully influences whether a fast synaptic transmission event triggers an action potential (Pampaloni *et al*, 2021). Provided the widespread distribution in the brain (Konno *et al*, 2014; Hepp *et al*, 2015; Nakamoto *et al*, 2020), GluD1<sub>R</sub> may contribute to pacemaking in



other neuronal populations, whether via intrinsic tonic current or following GqPCR activation.

## Conclusions

Our results show that GluD1<sub>R</sub> carries a G protein-independent tonic current that contributes to subthreshold neuronal excitation in the dorsal raphe nucleus. While the cause of tonic GluD1<sub>R</sub> current remains to be resolved, we identified an important part of our recording conditions that support measurement of this current—maintaining extracellular calcium at a physiological level (1.2 mM, Forsberg *et al*, 2019). Increasing extracellular calcium above 2 mM, which is standard to many artificial cerebral spinal fluids, reduced GluD1<sub>R</sub> unitary current and the magnitude of tonic GluD1<sub>R</sub> by ~50%.

Many studies have demonstrated the “non-ionic” functions of GluD1<sub>R</sub> in synapse formation and composition that require binding to presynaptic neurexins and secreted cerebellins (Tao *et al*, 2018; Dai *et al*, 2021). Work by Lemoine *et al* (2020) using HEK-293T cells expressing GluD2<sub>R</sub> indicates that stabilization of GluD2<sub>R</sub> in a trans-synaptic complex with presynaptic neurexins and secreted cerebellins is not required strictly for GPCR-stimulated and tonic GluD2<sub>R</sub> current, in contrast to recent observations with glycine-gated GluD2<sub>R</sub> current (Carrillo *et al*, 2021). But interestingly, genetic deletion of cerebellin-2 from dorsal raphe produces hyperactivity, hyperaggression, and compulsive behaviors in mice (Seigneur *et al*, 2021) that are similar to behaviors observed after global deletion of GluD1<sub>R</sub> (Yadav *et al*, 2012; Gupta *et al*, 2015). Further, genetic deletion of cerebellin-2 from dorsal raphe reduces serotonin levels in projection areas (Seigneur *et al*, 2021). However, future work will be needed to determine whether GluD1<sub>R</sub> ion channel function is potentiated by mechanical stabilization in the trans-synaptic complex or with other accessory proteins.

## Materials and Methods

### Animals

All studies were conducted in accordance with the University of Iowa with the approval of the University of Iowa Institutional Animal Care and Use Committee. Male and female wild-type C57BL/6J (> 2 months old, The Jackson Laboratory, #000664) mice were used. Mice were group-housed on a 12:12 h light cycle.

### Brain slice preparation and electrophysiological recordings

Brain slices and electrophysiological recordings were made as previously described (Khamma *et al*, 2022). In brief, mice were deeply anesthetized with isoflurane and euthanized by decapitation. Brains were removed and placed in warmed and bubbled (95/5% O<sub>2</sub>/CO<sub>2</sub>) modified Krebs' buffer containing (in mM): 126 NaCl, 2.5 KCl, 1.2 MgCl<sub>2</sub>, 1.2 CaCl<sub>2</sub>, 1.2 NaH<sub>2</sub>PO<sub>4</sub>, 21.5 NaHCO<sub>3</sub>, and 11 D-glucose with 5 μM MK-801 to reduce excitotoxicity and increase slice viability. In the same solution, coronal dorsal raphe slices (240 μm) were obtained using a vibrating microtome (Leica VT1000S) and incubated at 28°C > 30 min prior to recording.

Electrophysiological recordings were made in modified Krebs' buffer containing NBQX (3 μM) at 35°C with Multiclamp 200B and 700B amplifiers (Molecular Devices), Digidata 1440A and 1550B A/D converters (Molecular Devices), and Clampex software (Molecular Devices) with borosilicate glass electrodes (World Precision Instruments) wrapped with Parafilm to reduce pipette capacitance. Pipette resistances were 3.8–4.5 MΩ when filled with an internal solution containing, (in mM) 104.56 K-methylsulfate, 3.73 KCl, 5.3 NaCl, 4.06 MgCl<sub>2</sub>, 4.06 CaCl<sub>2</sub>, 7.07 HEPES (K), 3.25 BAPTA (K4), 0.26 GTP (sodium salt), 4.87 ATP (sodium salt), 4.59 creatine phosphate (sodium salt), pH 7.24 with KOH, mOsm ~274, for whole-cell patch-clamp recordings. Current–voltage relationships of tonic GluD1<sub>R</sub> current were determined using voltage ramps from –120 to 10 mV (1 mV/10 ms) including a voltage-gated sodium channel blocker, QX-314 (2 mM) in the internal solution. Current–voltage relationships of GIRK currents were determined using voltage ramps from –50 mV to –130 mV (–0.8 mV/ms). Synaptic currents were evoked on 90-s intervals by applying brief pulses (0.5 ms, 60 Hz) of electrical stimulation to the brain slice via a borosilicate glass monopolar stimulating electrode (World Precision Instruments) placed within 200 μm of the recorded neuron in the presence of GluN (MK-801), GluA/GluK (NBQX, 3 μM), GABA<sub>A</sub> (picrotoxin, 100 μM), and 5-HT1a (WAY-100635, 300 nM) receptor blockers to isolate the α1-A<sub>R</sub>-EPSC. Series resistance was monitored throughout the experiment. Reported voltages are corrected for a liquid junction potential of –8 mV between the internal and external solution. All drugs were applied via the patch pipette or by bath application. Noradrenaline was applied in the presence of an α2-adrenergic antagonist, idazoxan (1 μM).

### Materials

MK-801, NASPM, NBQX, noradrenaline, and prazosin were obtained from Tocris. All other reagents were from Sigma-Aldrich.

### Experimental design and statistical analysis

Data were analyzed using Clampfit 10.7 and 11.1 (Molecular Devices) or Igor-Pro 6.37 (Wavemetrics) with DataAccess (Bruxon Corporation) software and are presented in representative traces, scatter plots, and bar graphs with means ± SEM. Unless otherwise noted, *n* = number of cells as biological replicates. The investigators were not blind to the experimental conditions. To estimate sample size, we conducted power analyses ( $\alpha = 0.05$ ,  $\beta = 0.2$ ) based on detecting a 30% change in α1-A<sub>R</sub>-EPSC parameters or a 20 pA change in whole-cell current using standard deviations from published data with similar effect sizes (Gantz *et al*, 2020). Tonic current was measured as the peak of the NASPM-induced current minus the whole-cell current prior to NASPM application. Reversal potentials were determined using linear fit of the averaged data accounting for scatter among the replicates using at least one data point above and two below where the current reversed polarity. Significant differences were determined via Wilcoxon matched-pairs signed rank or two-way ANOVA tests for within-group comparisons and Mann–Whitney or Kruskal–Wallis tests for between-group comparisons. A difference of *P* < 0.05 was considered significant. Exact values are reported unless *P* < 0.0001 or > 0.999. Statistical analysis was performed using GraphPad Prism (GraphPad Software, Inc.).

## Data availability

Data have not been deposited in public databases, but are available upon request.

**Expanded View** for this article is available [online](#).

## Acknowledgements

We thank Holly S. Hake for critical reading and comments on the manuscript. This research was funded by awards from the Roy J. and Lucille A. Carver College of Medicine, University of Iowa, and Roy J. Carver Charitable Trust to SCG.

## Author contributions

**Daniel S Copeland:** Data curation; formal analysis; investigation; visualization; writing – original draft; writing – review and editing. **Alegha Gugel:** Data curation; formal analysis; investigation; writing – original draft; writing – review and editing. **Stephanie C Gantz:** Conceptualization; data curation; formal analysis; supervision; funding acquisition; investigation; visualization; methodology; writing – original draft; writing – review and editing.

## Disclosure and competing interests statement

The authors declare that they have no conflict of interest.

## References

- Ady V, Perroy J, Tricoire L, Piochon C, Dadak S, Chen X, Dusart I, Fagni L, Lambolez B, Levenes C (2013) Type 1 metabotropic glutamate receptors (mGlu1) trigger the gating of GluD2 delta glutamate receptors. *EMBO Rep* 15: 103–109
- Araki K, Meguro H, Kushiya E, Takayama C, Inoue Y, Mishina M (1993) Selective expression of the glutamate receptor channel delta 2 subunit in cerebellar Purkinje cells. *Biochem Biophys Res Commun* 197: 1267–1276
- Baraban JM, Wang RY, Aghajanian G (1978) Reserpine suppression of dorsal raphe neuronal firing: mediation by adrenergic system. *Eur J Pharmacol* 52: 27–36
- Benamer N, Marti F, Luján R, Hepp R, Aubier TG, Dupin AAM, Frébourg G, Pons S, Maskos U, Faure P et al (2018) GluD1, linked to schizophrenia, controls the burst firing of dopamine neurons. *Mol Psychiatry* 23: 691–700
- Bond RA, Iljerman AP (2006) Recent developments in constitutive receptor activity and inverse agonism, and their potential for GPCR drug discovery. *Trends Pharmacol Sci* 27: 92–96
- Brown RE, Sergeeva OA, Eriksson KS, Haas HL (2002) Convergent excitation of dorsal raphe serotonin neurons by multiple arousal systems (orexin/hypocretin, histamine and noradrenaline). *J Neurosci* 22: 8850–8859
- Carrillo E, Gonzalez CU, Berka V, Jayaraman V (2021) Delta glutamate receptors are functional glycine- and D-serine-gated cation channels in situ. *Sci Adv* 7: eabk2200
- Castillo PE, Malenka RC, Nicoll RA (1997) Kainate receptors mediate a slow postsynaptic current in hippocampal CA3 neurons. *Nature* 388: 182–186
- Chiu DN, Jahr CE (2017) Extracellular glutamate in the nucleus accumbens is nanomolar in both synaptic and non-synaptic compartments. *Cell Rep* 18: 2576–2583
- Chua HC, Wulf M, Weidling C, Rasmussen LP, Pless SA (2020) The NALCN channel complex is voltage sensitive and directly modulated by extracellular calcium. *Sci Adv* 6: eaaz3154
- Coombs ID, Soto D, McGee TP, Gold MG, Farrant M, Cull-Candy SG (2019) Homomeric GluA2(R) AMPA receptors can conduct when desensitized. *Nat Commun* 10: 4312
- Dadak S, Bouquier N, Goyet E, Fagni L, Levenes C, Perroy J (2017) mGlu1 receptor canonical signaling pathway contributes to the opening of the orphan GluD2 receptor. *Neuropharmacology* 115: 92–99
- Dai J, Patzke C, Liakath-Ali K, Seigneur E, Südhof TC (2021) GluD1 is a signal transduction device disguised as an ionotropic receptor. *Nature* 595: 1–21
- Eggermann E, Bucurenciu I, Goswami SP, Jonas P (2011) Nanodomain coupling between Ca<sup>2+</sup> channels and sensors of exocytosis at fast mammalian synapses. *Nat Rev Neurosci* 13: 7–21
- Egorov AV, Hamam BN, Fransén E, Hasselmo ME, Alonso AA (2002) Graded persistent activity in entorhinal cortex neurons. *Nature* 420: 173–178
- Egorov AV, Schumacher D, Medert R, Birnbaumer L, Freichel M, Draguhn A (2019) TRPC channels are not required for graded persistent activity in entorhinal cortex neurons. *Hippocampus* 29: 1038–1048
- Forsberg M, Seth H, Björefeldt A, Lyckenvik T, Andersson M, Wasling P, Zetterberg H, Hanse E (2019) Ionized calcium in human cerebrospinal fluid and its influence on intrinsic and synaptic excitability of hippocampal pyramidal neurons in the rat. *J Neurochem* 149: 452–470
- Fossati M, Assendorp N, Gemin O, Colasse S, Dingli F, Arras G, Loew D, Charrier C (2019) Trans-synaptic signaling through the glutamate Receptor Delta-1 mediates inhibitory synapse formation in cortical pyramidal neurons. *Neuron* 104: 1081–1094
- Gantz SC, Bunzow JR, Williams JT (2013) Spontaneous inhibitory synaptic currents mediated by a G protein-coupled receptor. *Neuron* 78: 807–812
- Gantz SC, Moussawi K, Hake HS (2020) Delta glutamate receptor conductance drives excitation of mouse dorsal raphe neurons. *Elife* 9: e56054
- Gawande DY, Shelkar GP, Liu J, Ayala AD, Pavuluri R, Choi D, Smith Y, Dravid SM (2021) Glutamate Delta-1 receptor regulates inhibitory neurotransmission in the nucleus Accumbens Core and anxiety-like behaviors. *Mol Neurobiol* 58: 4787–4801
- Gawande DY, Narasimhan KKS, Bhatt JM, Pavuluri R, Kesharwani V, Suryavanshi PS, Shelkar GP, Dravid SM (2022) Glutamate delta 1 receptor regulates autophagy mechanisms and affects excitatory synapse maturation in the somatosensory cortex. *Pharmacol Res* 178: 106144
- Gupta SC, Yadav R, Pavuluri R, Morley BJ, Stairs DJ, Dravid SM (2015) Essential role of GluD1 in dendritic spine development and GluN2B to GluN2A NMDAR subunit switch in the cortex and hippocampus reveals ability of GluN2B inhibition in correcting hyperconnectivity. *Neuropharmacology* 93: 274–284
- Hansen KB, Naur P, Kurtkaya NL, Kristensen AS, Gajhede M, Kastrop JS, Traynelis SF (2009) Modulation of the dimer interface at ionotropic glutamate-like receptor 2 by D-serine and extracellular calcium. *J Neurosci* 29: 907–917
- Hanson E, Armbruster M, Lau LA, Sommer ME, Klaft Z-J, Swanger SA, Traynelis SF, Moss SJ, Noubary F, Chadchankar J et al (2019) Tonic activation of GluN2C/GluN2D-containing NMDA receptors by ambient glutamate facilitates cortical interneuron maturation. *J Neurosci* 39: 3611–3626
- Hein P, Goepel M, Cotecchia S, Michel MC (2001) A quantitative analysis of antagonism and inverse agonism at wild-type and constitutively active hamster  $\alpha 1B$ -adrenoceptors. *Naunyn Schmiedeberg Arch Pharmacol* 363: 34–39
- Hepp R, Hay YA, Aguado C, Luján R, Dauphinot L, Potier MC, Nomura S, Poirel O, Mestikawy SE, Lambolez B et al (2015) Glutamate receptors of the delta family are widely expressed in the adult brain. *Brain Struct Funct* 220: 2797–2815

- Hoover AH, Pavuluri R, Shelkar GP, Dravid SM, Smith Y, Villalba RM (2021) Ultrastructural localization of glutamate delta 1 (GluD1) receptor immunoreactivity in the mouse and monkey striatum. *J Comp Neurol* 529: 1703–1718
- Hubbard CM, Redpath GT, Macdonald TL, VandenBerg SR (1989) Modulatory effects of aluminum, calcium, lithium, magnesium, and zinc ions on [3H]MK-801 binding in human cerebral cortex. *Brain Res* 486: 170–174
- Jackson AC, Yao GL, Bean BP (2004) Mechanism of spontaneous firing in dorsomedial suprachiasmatic nucleus neurons. *J Neurosci* 24: 7985–7998
- Khalik ZM, Bean BP (2010) Pacemaking in dopaminergic ventral tegmental area neurons: depolarizing drive from background and voltage-dependent sodium conductances. *J Neurosci* 30: 7401–7413
- Khamma JK, Copeland DS, Hake HS, Gantz SC (2022) Spatiotemporal control of noradrenaline-dependent synaptic transmission in mouse dorsal raphe serotonin neurons. *J Neurosci* 42: 968–979
- Koike M, Iino M, Ozawa S (1997) Blocking effect of 1-naphthyl acetyl spermine on Ca(2+)-permeable AMPA receptors in cultured rat hippocampal neurons. *Neurosci Res* 29: 27–36
- Konno K, Matsuda K, Nakamoto C, Uchigashima M, Miyazaki T, Yamasaki M, Sakimura K, Yuzaki M, Watanabe M (2014) Enriched expression of GluD1 in higher brain regions and its involvement in parallel fiber-interneuron synapse formation in the cerebellum. *J Neurosci* 34: 7412–7424
- Kramer PF, Williams JT (2016) Calcium release from stores inhibits GIRK. *Cell Rep* 17: 3246–3255
- Landsend AS, Amiry-Moghaddam M, Matsubara A, Bergersen L, Usami S, Wenthold RJ, Ottersen OP (1997) Differential localization of  $\delta$  glutamate receptors in the rat cerebellum: coexpression with AMPA receptors in parallel fiber–spine synapses and absence from climbing fiber–spine synapses. *J Neurosci* 17: 834–842
- Lemoine D, Mondoloni S, Tange J, Lambalez B, Faure P, Taly A, Tricoire L, Mourot A (2020) Probing the ionotropic activity of glutamate GluD2 receptor in HEK cells with genetically-engineered photopharmacology. *Elife* 9: e59026
- Li K, Abbott SBC, Shi Y, Eggan P, Gonye EC, Bayliss DA (2021) TRPM4 mediates a subthreshold membrane potential oscillation in respiratory chemoreceptor neurons that drives pacemaker firing and breathing. *Cell Rep* 34: 108714
- Lomeli H, Sprengel R, Laurie DJ, Kohr G, Herb A, Seeburg PH, Wisden W (1993) The rat delta-1 and delta-2 subunits extend the excitatory amino acid receptor family. *FEBS Lett* 315: 318–322
- Lopes JP, Cunha RA (2019) What is the extracellular calcium concentration within brain synapses? *J Neurochem* 149: 435–437
- Loucif AJC, Bonnavion P, Macri B, Golmard J-L, Boni C, Melfort M, Leonard G, Lesch K-P, Adrien J, Jacquin TD (2006) Gender-dependent regulation of G-protein-gated inwardly rectifying potassium current in dorsal raphe neurons in knock-out mice devoid of the 5-hydroxytryptamine transporter. *J Neurobiol* 66: 1475–1488
- Lu B, Su Y, Das S, Liu J, Xia J, Ren D (2007) The neuronal channel NALCN contributes resting sodium permeability and is required for normal respiratory rhythm. *Cell* 129: 371–383
- Lu B, Su Y, Das S, Wang H, Wang Y, Liu J, Ren D (2009) Peptide neurotransmitters activate a cation channel complex of NALCN and UNC-80. *Nature* 457: 741–744
- Lu B, Zhang Q, Wang H, Wang Y, Nakayama M, Ren D (2010) Extracellular calcium controls background current and neuronal excitability via an UNC79-UNC80-NALCN Cation Channel complex. *Neuron* 68: 488–499
- Lu H-W, Balmer TS, Romero GE, Trussell LO (2017) Slow AMPAR synaptic transmission is determined by Stargazin and glutamate transporters. *Neuron* 96: 73–80
- Maki BA, Popescu GK (2014) Extracellular Ca<sup>2+</sup> ions reduce NMDA receptor conductance and gating. *J Gen Physiol* 144: 379–392
- McKay S, Bengtson CP, Bading H, Wyllie DJA, Hardingham GE (2013) Recovery of NMDA receptor currents from MK-801 blockade is accelerated by Mg<sup>2+</sup> and memantine under conditions of agonist exposure. *Neuropharmacology* 74: 119–125
- Meur KL, Galante M, Angulo MC, Audinat E (2007) Tonic activation of NMDA receptors by ambient glutamate of non-synaptic origin in the rat hippocampus. *J Physiol* 580: 373–383
- Misra C, Brickley SG, Wyllie DJA, Cull-Candy SG (2000) Slow deactivation kinetics of NMDA receptors containing NR1 and NR2D subunits in rat cerebellar Purkinje cells. *J Physiol* 525: 299–305
- Nakamoto C, Konno K, Miyazaki T, Nakatsukasa E, Natsume R, Abe M, Kawamura M, Fukazawa Y, Shigemoto R, Yamasaki M et al (2020) Expression mapping, quantification, and complex formation of GluD1 and GluD2 glutamate receptors in adult mouse brain. *J Comp Neurol* 528: 1003–1027
- Naur P, Hansen KB, Kristensen AS, Dravid SM, Pickering DS, Olsen L, Vestergaard B, Egebjerg J, Gajhede M, Traynelis SF et al (2007) Ionotropic glutamate-like receptor delta2 binds D-serine and glycine. *Proc Natl Acad Sci USA* 104: 14116–14121
- Pampaloni NP, Riva I, Carbone A, Plested AJR (2021) Slow AMPA receptors in hippocampal principal cells. *Cell Rep* 35: 109496
- Pfaffinger PJ, Martin JM, Hunter DD, Nathanson NM, Hille B (1985) GTP-binding proteins couple cardiac muscarinic receptors to a K channel. *Nature* 317: 536–538
- Philippart F, Khalik ZM (2018) Gi/o protein-coupled receptors in dopamine neurons inhibit the sodium leak channel NALCN. *Elife* 7: e40984
- Prézeau L, Gomez J, Ahern S, Mary S, Galvez T, Bockaert J, Pin JP (1996) Changes in the carboxyl-terminal domain of metabotropic glutamate receptor 1 by alternative splicing generate receptors with differing agonist-independent activity. *Mol Pharmacol* 49: 422–429
- Quallo T, Alkhatib O, Gentry C, Andersson DA, Bevan S (2017) G protein  $\beta\gamma$  subunits inhibit TRPM3 ion channels in sensory neurons. *Elife* 6: e26138
- Raman IM, Gustafson AE, Padgett D (2000) Ionic currents and spontaneous firing in neurons isolated from the cerebellar nuclei. *J Neurosci* 20: 9004–9016
- Ren D (2011) Sodium leak channels in neuronal excitability and rhythmic behaviors. *Neuron* 72: 899–911
- Reynolds IJ, Miller RJ (1988) Multiple sites for the regulation of the N-methyl-D-aspartate receptor. *Mol Pharmacol* 33: 581–584
- Rodriguez-Contreras D, Condon AF, Buck DC, Asad N, Dore TM, Verbeek DS, Tijssen MAJ, Shinde U, Williams JT, Neve KA (2021) Signaling-biased and constitutively active dopamine D2 receptor variant. *ACS Chem Neurosci* 12: 1873–1884
- Sah P, Hestrin S, Nicoll RA (1989) Tonic activation of NMDA receptors by ambient glutamate enhances excitability of neurons. *Science* 246: 815–818
- Seigneur E, Wang J, Dai J, Polepalli J, Südhof TC (2021) Cerebellin-2 regulates a serotonergic dorsal raphe circuit that controls compulsive behaviors. *Mol Psychiatry* 26: 7509–7521
- Shen Y, Rampino MAF, Carroll RC, Nawy S (2012) G-protein-mediated inhibition of the Trp channel TRPM1 requires the G dimer. *Proc Natl Acad Sci USA* 109: 8752–8757
- Svensson TH, Bunney BS, Aghajanian GK (1975) Inhibition of both noradrenergic and serotonergic neurons in brain by the alpha-adrenergic agonist clonidine. *Brain Res* 92: 291–306

- Taddese A, Bean BP (2002) Subthreshold sodium current from rapidly inactivating sodium channels drives spontaneous firing of Tuberomammillary neurons. *Neuron* 33: 587–600
- Tao W, Díaz-Alonso J, Sheng N, Nicoll RA (2018) Postsynaptic  $\delta 1$  glutamate receptor assembles and maintains hippocampal synapses via Cbln2 and neurexin. *Proc Natl Acad Sci USA* 115: E5373–E5381
- van den Top M, Lee K, Whyment AD, Blanks AM, Spanswick D (2004) Orexin-sensitive NPY/AgRP pacemaker neurons in the hypothalamic arcuate nucleus. *Nat Neurosci* 7: 493–494
- Vandermaelen CP, Aghajanian GK (1983) Electrophysiological and pharmacological characterization of serotonergic dorsal raphe neurons recorded extracellularly and intracellularly in rat brain slices. *Brain Res* 289: 109–119
- Yadav R, Rimerman R, Scofield MA, Dravid SM (2011) Mutations in the transmembrane domain M3 generate spontaneously open orphan glutamate  $\delta 1$  receptor. *Brain Res* 1382: 1–8
- Yadav R, Gupta SC, Hillman BG, Bhatt JM, Stairs DJ, Dravid SM (2012) Deletion of glutamate delta-1 receptor in mouse leads to aberrant emotional and social behaviors. *PLoS ONE* 7: e32969
- Yamada-Hanff J, Bean BP (2013) Persistent sodium current drives conditional pacemaking in CA1 pyramidal neurons under muscarinic stimulation. *J Neurosci* 33: 15011–15021
- Zhang X, Mak S, Li L, Parra A, Denlinger B, Belmonte C, McNaughton PA (2012) Direct inhibition of the cold-activated TRPM8 ion channel by  $G\alpha_q$ . *Nat Cell Biol* 14: 851–858



**License:** This is an open access article under the terms of the [Creative Commons Attribution](#) License, which permits use, distribution and reproduction in any medium, provided the original work is properly cited.